



## ORIGINAL ARTICLE

# EGFR tyrosine kinase inhibitor HS-10182 increases radiation sensitivity in non-small cell lung cancers with EGFR T790M mutation

Yang Chen<sup>1\*</sup>, Youyou Wang<sup>1\*</sup>, Lujun Zhao<sup>1</sup>, Ping Wang<sup>1</sup>, Jifeng Sun<sup>1</sup>, Rudi Bao<sup>2</sup>, Chenghai Li<sup>2</sup>, Ningbo Liu<sup>1</sup>

<sup>1</sup>Department of Radiation Oncology, Tianjin Medical University Cancer Institute and Hospital, National Clinical Research Center for Cancer; Key Laboratory of Cancer Prevention and Therapy, Tianjin; Tianjin's Clinical Research Center for Cancer, Tianjin 300060, China; <sup>2</sup>Jiangsu Hansoh Pharmaceutical Co., Ltd, Lianyungang 222069, China

### ABSTRACT

**Objective:** To investigate the potential of HS-10182, a second-generation epidermal growth factor receptor tyrosine kinase inhibitor (EGFR-TKI), as a radiosensitizer in non-small cell lung cancer (NSCLC).

**Methods:** Two cell lines of NSCLCs, A549 that possesses wild-type (WT) EGFRs and H1975 that possesses EGFR L858R/T790M double mutations, were treated with HS-10182 at various concentrations, and cell viabilities were determined using the MTS assay. The cells were tested by clonogenic survival assays to identify the radiosensitivity of both groups. Western blot was performed to analyze the expression of phosphorylated EGFR, AKT, DNA-dependent protein kinase, and catalytic subunit (DNA-PKcs) proteins. Immunofluorescence analyses were performed to examine the formation and changes in nuclear  $\gamma$ -H2AX foci. Cell apoptosis was examined by flow cytometry and Western blots for cleaved caspase-3, -8, -9, and cleaved poly ADP-ribose polymerase (PARP). Furthermore, we established xenograft models in mice and the effects of different treatments on tumor growth were then assessed.

**Results:** Clonogenic survival assays revealed that HS-10182 significantly enhanced the radiosensitivity of H1975 cells but not A549 cells [dose enhancement ratios (DERs)=2.36 ( $P < 0.05$ ) vs. 1.43 ( $P > 0.05$ )]. Western blot results showed that HS-10182 increased the levels of cleaved caspase-3, -8, -9, and cleaved PARP in H1975 cells but not in A549 cells. In addition, flow cytometry analysis showed that HS-10182 enhanced irradiation-induced apoptosis in H1975. Immunofluorescence results found that HS-10182 increased the average number of  $\gamma$ -H2AX foci after irradiation in H1975 cells, but not in A549 cells. Combined radiation and HS-10182 treatment increased the expression of DNA-PKcs but this increase was more significant in H1975 cells than in A549 cells. Moreover, HS-10182 suppressed the increased expression of Rad50 in H1975 cells in response to irradiation. *In vivo* experiments found that the combined therapy significantly inhibited tumor growth.

**Conclusions:** HS-10182 enhances the radiosensitivity of H1975 cells which is possibly because that HS-10182 could enhance irradiation-induced apoptosis, increase irradiation-induced DNA damage, and cause a delay in DNA damage repair. Our findings suggest that radiotherapy combined HS-10182 is a novel treatment for lung cancer cells which have acquired the T790M mutation. HS-10182 could be brought to the clinic as a radiosensitizer in NSCLCs with the EGFR T790M mutation.

### KEYWORDS

HS-10182; radiosensitization; NSCLC; EGFR-TKI; T790M mutation; radiosensitivity

## Introduction

Epidermal growth factor receptor (EGFR) is a member of the ErbB family and is an important transmembrane receptor that mediates tyrosine kinase activity. Signaling that is

activated at downstream of EGFR can direct cellular migration, adhesion, proliferation, differentiation, and apoptosis<sup>1</sup>. Consequently, EGFR plays a fundamental role in the development and growth of many types of human tumor cells<sup>2</sup>. In some tumors, EGFR is mutated or increased in expression<sup>3</sup>. These events are often associated with increased resistance to radiation treatment<sup>4</sup>.

Non-small cell lung cancer (NSCLC) constitutes approximately 85% of all lung cancer cases and it has the highest mortality rate of all cancers worldwide<sup>5</sup>. Approximately 50% of NSCLC patients receive radiation therapy (RT) during the course of the disease<sup>6</sup>. For NSCLC patients that carry mutations in EGFR, EGFR tyrosine kinase

\*These authors have contributed equally to this work.

Correspondence to: Ningbo Liu

E-mail: tj\_liuningbo@163.com

Received September 2, 2017; accepted December 28, 2017.

Available at www.cancerbiomed.org

Copyright © 2018 by Cancer Biology & Medicine

inhibitors (EGFR-TKIs) are widely used<sup>7</sup>. However, for NSCLC patients, a combination therapy of radiation and EGFR-TKI is uncommon at present in our clinical practice. A number of preclinical studies have reported that EGFR-TKIs, such as erlotinib, can enhance radiation response<sup>8</sup>. However, it remains unclear whether EGFR-TKIs can enhance the radiosensitivity of NSCLC patients carrying an EGFR T790M mutation to increase tumor control. HS-10182 is a second-generation EGFR-TKI that was used in the present study to treat human NSCLC cells and to investigate its potential as a radiosensitizer.

In this study, we examined how HS-10182 affects the radiosensitivity of H1975 cells carrying an EGFR L858R/790M double mutation *in vitro*. An evaluation of HS-10182 in an *in vivo* model was also conducted. We compared how the combined RT and HS-10182 treatment affected tumor growth relative to each mono-treatment alone. To our knowledge, this is the first study to examine whether a new-generation of EGFR-TKI can induce tumor radiosensitization and increase tumor control. This study is an important step in determining whether HS-10182 has the potential to serve as a radiosensitizer in the treatment of NSCLCs that carry an EGFR T790M mutation.

## Materials and methods

### Cell lines

A549 and H1975 cells were provided by Tianjin Medical University Cancer Institute and Hospital. These cells were cultured in RPMI-1640 medium supplemented with 10% fetal bovine serum (FBS), 100 U/mL penicillin, and 100 U/mL streptomycin and were maintained at 37°C in a humidified atmosphere with 5% CO<sub>2</sub>. Cells were cultured overnight to reach 50%–70% confluence before being divided into 4 treatment groups: untreated normal control (NC), HS-10182 (HS), radiotherapy (RT), and radiotherapy + HS-10182 (RT+HS). Radiotherapy included 6 MV X-ray irradiation that was administered at 6 Gy/fraction. For the RT+HS group, cells were treated with HS-10182 for 2 h and then they received one dose of ionizing radiation at 6 Gy/fraction.

### Proliferation assay

Cell proliferation was assayed with a CellTiter 96® Aqueous Non-Radioactive Cell Proliferation assay (Promega, Madison, WI, USA). Briefly, approximately  $2 \times 10^3$  cells/well were plated in 96-well plates and grown overnight. The cells were then treated with various concentrations (0–1600 nM) of HS-10182 for 24, 48, 72, or 96 h. At each timepoint, 20  $\mu$ L

of MTS reagent was added to each well and the plates were incubated in the dark at 37°C. After 3 h, an absorbance value for each well was measured at 490 nm using a microplate reader (Bio-Rad Laboratories, Hercules, CA, USA). Cell viability was calculated by dividing the treated cell absorbances by the absorbances of the untreated cells. IC<sub>20</sub> and IC<sub>50</sub> values were calculated based on the concentration of drug that was required to obtain 20% and 50% of the maximal cell viability, respectively.

### Western blot analysis

Cells were collected, washed with cold phosphate-buffered saline (PBS), and lysed in RIPA buffer. Protein concentrations were determined with a microplate reader (Bio-Rad Laboratories) and absorbance measurements were taken at 562 nm. Protein lysates were separated using SDS-PAGE (using 8%–12% SDS gels) and transferred to polyvinylidene difluoride (PVDF) membranes. The membranes were blocked in 5% nonfat dry milk in Tris-buffered saline and Tween 20 (TBST) for 2 h at room temperature. The membranes were then incubated overnight at 4°C with primary antibodies purchased from Cell Signaling Technology (Danvers, MA, USA) that recognize: phospho-EGFR (#3777, 1:1000), EGFR (#4267, 1:1000), phospho-AKT (#9271, 1:1000), AKT (#4691, 1:1000), caspase-3 (#9665, 1:1000), PARP (#9542, 1:1000), caspase-8 (#9746, 1:1000), caspase-9 (#9508, 1:1000), DNA-PKcs (#12311, 1:1000), Rad50 (#3427, 1:1000), Ku70 (#4588, 1:1000),  $\gamma$ -H2AX (#9718, 1:1000), and  $\beta$ -actin (#3700, 1:1000). The next day, the membranes were incubated with horseradish peroxidase-conjugated goat anti-rabbit/mouse secondary antibodies (1:2000; Cell Signal Technology) as appropriate. After 1 h at room temperature, band intensities were quantified and analyzed with Quantity One 1 Image Analysis Software (Bio-Rad).

### Clonogenic survival assay

Different numbers of A549 and H1975 lung cancer cells were cultured in 6-well plates and treated with various doses of radiation (0, 2, 4, and 6 Gy) following a 2 h pretreatment with or without HS-10182 on day 1. The cells were allowed to grow and form colonies for approximately 14 d; the colonies that formed were fixed with methanol and stained with 0.5% crystal violet. Colonies with more than 50 cells were counted. The following formulas were used to calculate the indicated parameters: Plating Efficiency (PE) = numbers of colonies formed (control group)/numbers of cells plated  $\times$  100%; Surviving fractions (SF) = number of colonies formed/

[number of cells plated (irradiated group)  $\times$  plating efficiency (control group)]. Dose enhancement ratios (DERs) were calculated based on the ratio of the 30% surviving fraction doses for the control group and the combination group.

### Flow cytometry analysis of cell cycle and apoptosis

To analyze the rates of cell apoptosis, a commercially available annexin V-FITC kit was used (BD Biosciences, Franklin Lakes, NJ, USA). Briefly, A549 and H1975 cells were plated in 6-well plates and were divided into the four treatment groups described above. After 24 h of treatment, cells were harvested by trypsinization, collected by centrifugation, and washed twice with cold PBS. Each sample of cells was then resuspended in 200  $\mu$ L 1 $\times$  binding buffer and subsequently incubated with 2  $\mu$ L annexin V-FITC and 2  $\mu$ L propidium iodide (PI). After an incubation period in the dark at room temperature for 15 min, the population of apoptotic cells in each cell sample was detected by flow cytometry within 1 h of completing the incubation period.

### Immunofluorescence (IF)

To detect  $\gamma$ -H2AX foci, DNA-PKcs, and Rad50 via IF, cells were plated on coverslips overnight. The cells were then treated with 6 Gy irradiation after a 2 h pretreatment with or without HS-10182 on day 2. After the cells were fixed in 4% paraformaldehyde at 4°C for various periods following irradiation, the cells were permeabilized in 0.2% TritonX-100 in PBS for 15 min at room temperature. The cells were then incubated in 5% bovine serum albumin (BSA) in PBS for 1 h at room temperature before being incubated with a rabbit anti- $\gamma$ -H2AX antibody (1:400, #9718, Cell Signaling Technology), mouse anti-DNA-PKcs antibody (1:100, #12311, Cell Signaling Technology), or mouse anti-Rad50 antibody (1:200, ab124682, Abcam, USA) overnight at 4°C. The next day, the cells were incubated with a fluorescently-labeled goat anti-rabbit/mouse secondary antibody (1:200; ZSGB-BIO, China) for 1 h at room temperature. DAPI staining (blue) was used to visualize DNA among the bound antibodies detected by confocal microscopy (OLYMPUS BX61, Japan) 150 cells from each experiment were randomly selected for counting  $\gamma$ -H2AX foci present in each nucleus. Data represent the average of three experiments.

### *In vivo* tumor growth assay

This study was performed in accordance with the relevant

guidelines and regulations and was approved by the ethical committee of Tianjin Medical University Cancer Institute and Hospital, China. Female Nu/Nu mice (6 weeks old, 16–18 g) were used for the xenograft experiments. Briefly, H1975 cells ( $1 \times 10^6$  cells in 0.2 mL normal saline) were injected subcutaneously into the right thigh of each mouse. When the average tumor volume reached 200 mm<sup>3</sup>, the mice were randomized into four groups to receive the following treatments: no treatment [control group (NC)]; HS-10182 (5 mg/kg per day, days 6–12); RT (10 Gy/5 fractions on days 8–12); and RT (10 Gy/5 fractions on days 8–12) + HS-10182 (5 mg/kg per day, days 6–12). Tumors were measured three times per week and tumor volumes were calculated as follows: volume = depth  $\times$  width  $\times$  length  $\times$  0.5.

### Immunohistochemistry

H1975 xenograft tumors were collected after two weeks of daily treatments. Briefly, the tumors were resected and frozen in 10% neutral buffered formalin. Sections from the tumors (4 mm thickness) were placed on tissue slides that had been prepared with a dewaxing step with xylene followed by dehydration with gradient ethanol and rehydration with PBS. The sections were immersed in 3% hydrogen peroxide for 20 min, then in 5% BSA for 30 min. The tissue slides were subsequently incubated with primary antibodies recognizing p-EGFR, EGFR, DNA-PKcs, Ki67, Rad50, or Ku70 (Cell Signaling Technology) for 60 min at room temperature and then at 4°C overnight. The next day, the sections were washed with PBS, incubated with a secondary antibody (PV-9000 ZSGB-BIO, China) for 30 min at 37°C, and then incubated with Diaminobenzidine (DAB). After the sections were counterstained with hematoxylin, they were air-dried, dehydrated, and observed under a microscope.

### Statistical analysis

Statistical analyses were performed by using Statistical Product and Service Solutions 18.0 software package (IBM Corporation, Armonk, NY, USA). Student's *t*-test was used for calculating the significance of the differences between the control and treatment groups. A *P*-value less than 0.05 was considered significant.

## Results

### Effect of HS-10182 on cell proliferation and EGFR signaling

As shown in **Figure 1**, the viability of the H1975 cells

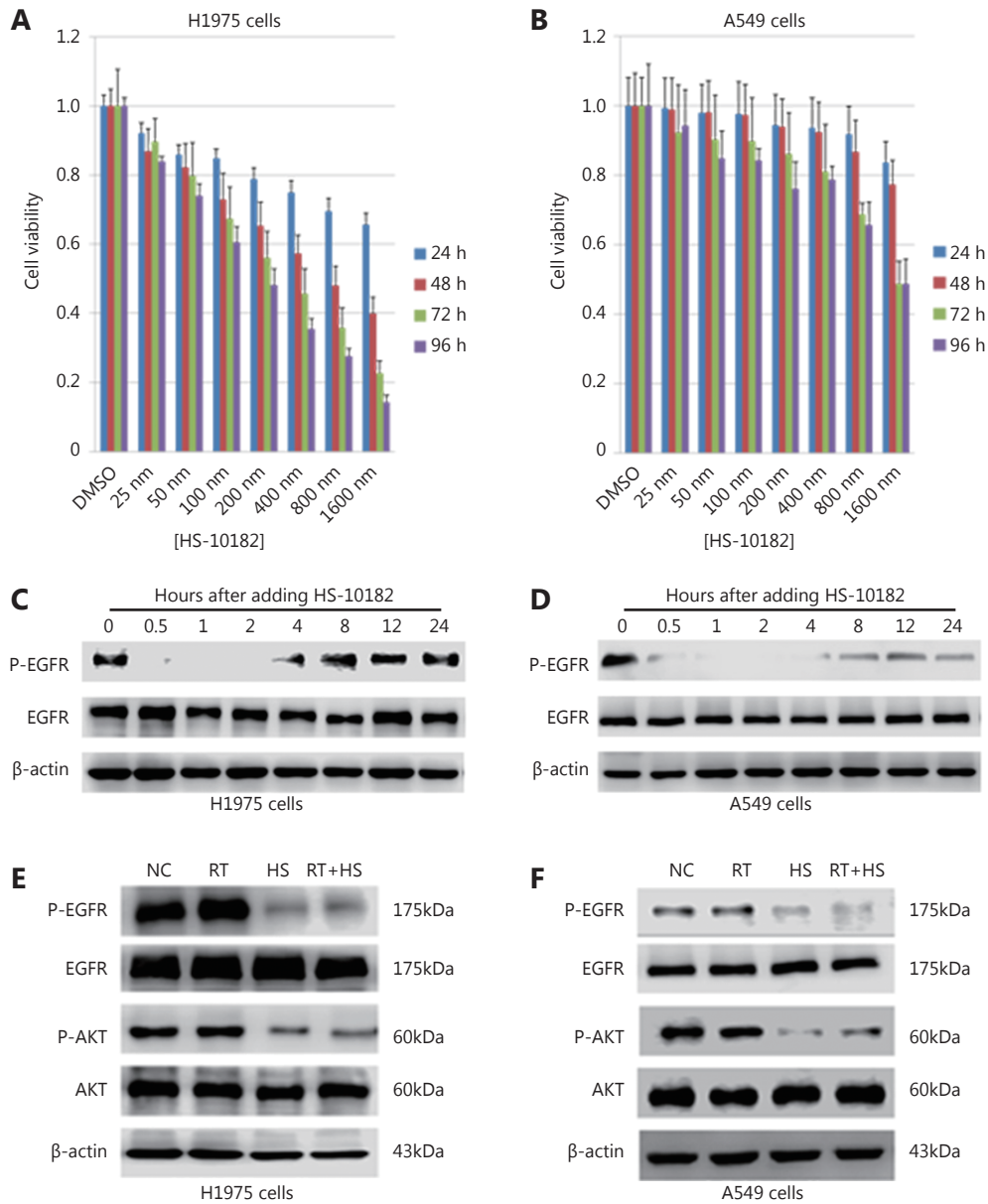


**Figure 1** Effect of HS-10182 on cell proliferation and EGFR signaling. H1975 (A) and A549 lung cancer cells (B) were exposed to the indicated concentrations of HS-10182 and MTS assays were performed 24, 48, 72, and 96 h after each treatment. Error bars indicate SD values from at least three independent experiments. Western blot of H1975 (C) and A549 cell lysates (D) was performed to detect levels of p-EGFR and total EGFR at various time points after the addition of HS-10182. Actin served as a loading control. Cell lysates were collected from H1975 (E) and A549 cells (F) that were treated with radiation (RT), 2 h with HS-10182 (HS), or a combination of both for 2 h (RT+HS). Levels of p-EGFR, total EGFR, p-AKT, and total AKT proteins were detected by Western blot. Detection of actin provided a loading control. NC, no treatment control group.

decreased with time and at higher doses of HS-10182, whereas A549 viability remained nearly unchanged. In the MTS assays (Figure 1A and B), the 48 h time point was selected for the calculation of  $IC_{50}$  values. The  $IC_{50}$  values for HS-10182 were 659 nM for the H1975 cell line and 1.6  $\mu$ M

for the A549 cell line. Thus, the NSCLC cells carrying the T790M mutation in EGFR were relatively sensitive to HS-10182 as compared with the cells that carried wild-type EGFR. To examine whether HS-10182 blocks EGFR signaling, levels of phosphorylated EGFR (p-EGFR) and total

EGFR were detected in both cell lines following the administration of HS-10182 at concentrations of 659 nM and 1.6  $\mu$ M, respectively. Lower levels of p-EGFR were initially detected after 30 min of HS-10182 treatment in both the H1975 and A549 cells. Approximately 4 h later, the levels of p-EGFR began to return to basal levels (Figure 1C and D). Several groups have reported that AKT signaling is activated by irradiation<sup>9</sup>. Therefore, the effects of HS-10182 on the phosphorylation of AKT (p-AKT) and total AKT were also investigated. Both cell lines were treated with HS-10182 in combination with 6 Gy of radiation. Levels of p-AKT were very high in the H1975 cells, whereas the levels of p-AKT were lower in the RT+HS group (Figure 1E). In contrast, no significant changes in the levels of p-AKT in the A549 cells were observed in any of the treatment groups (Figure 1F).

### HS-10182 significantly enhances the radiosensitivity of H1975 cells but not A549 cells

*In vitro* clonogenic assays were conducted to determine the

effect of HS-10182 on radiosensitivity. Both the H1975 and A549 cell lines formed colonies (Figure 2A and C). However, while the WT EGFR cell line, A549, exhibited significant tolerance to radiation with only minimal loss of colony-forming ability at 6 Gy, the H1975 cells carrying the EGFR L858R/T790M double mutation exhibited high radiosensitivity as compared with the unirradiated controls. Thus, HS-10182 significantly enhances the radiosensitivity of H1975 cells but not A549 cells. Furthermore, the dose enhancement ratio (DER) at survival fraction level 0.3 was 2.36 for the H1975 cells and 1.43 for the A549 cells (Figure 2B and D).

### HS-10182 enhances irradiation-induced apoptosis

Cleavage of caspase-8, caspase-9, caspase-3, and PARP to their active forms are very important events in cancer cell apoptosis<sup>10</sup>. Therefore, we assessed the levels of these apoptosis-related proteins in Western blot (Figure 3A). In extracts collected from H1975 cells, levels of cleaved caspase-

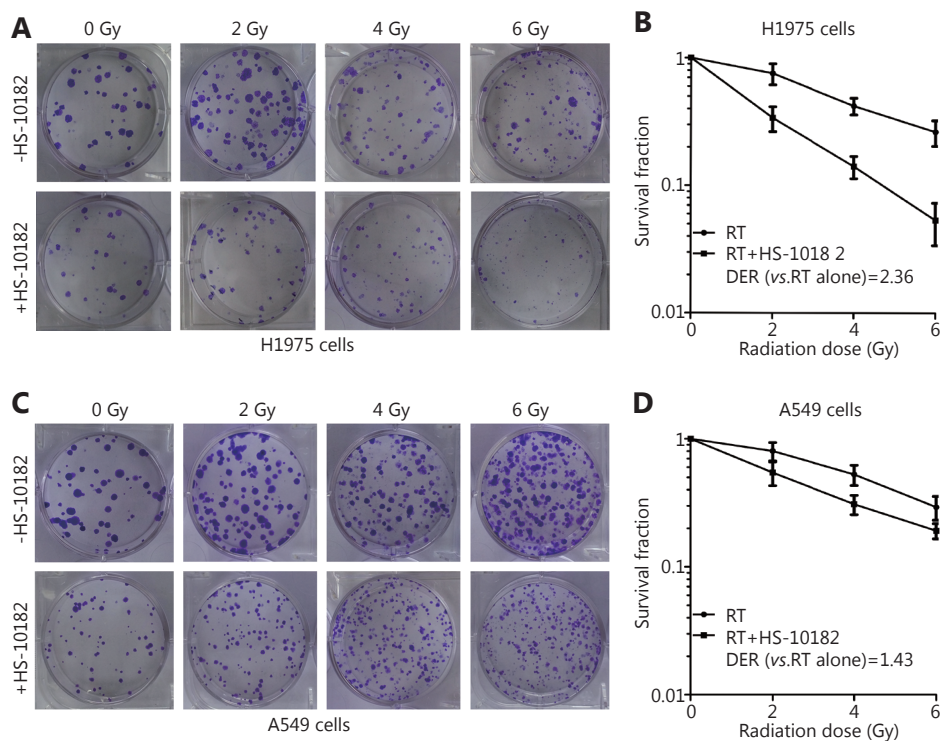


**Figure 2** HS-10182 significantly enhances the radiosensitivity of H1975 cells but not A549 cells. Clonogenic survival assays were performed for H1975 (A) and A549 cells (C) in the presence and absence of HS-10182 treatment in combination with various doses of radiation (0–6 Gy). The formation of clear colonies was subsequently observed. The corresponding clonogenic survival curves reveal that HS-10182 mediates a significant radiosensitizing effect in H1975 cells (B) but not in A549 cells (D). The results are expressed as the mean  $\pm$  SD values from three independent experiments.

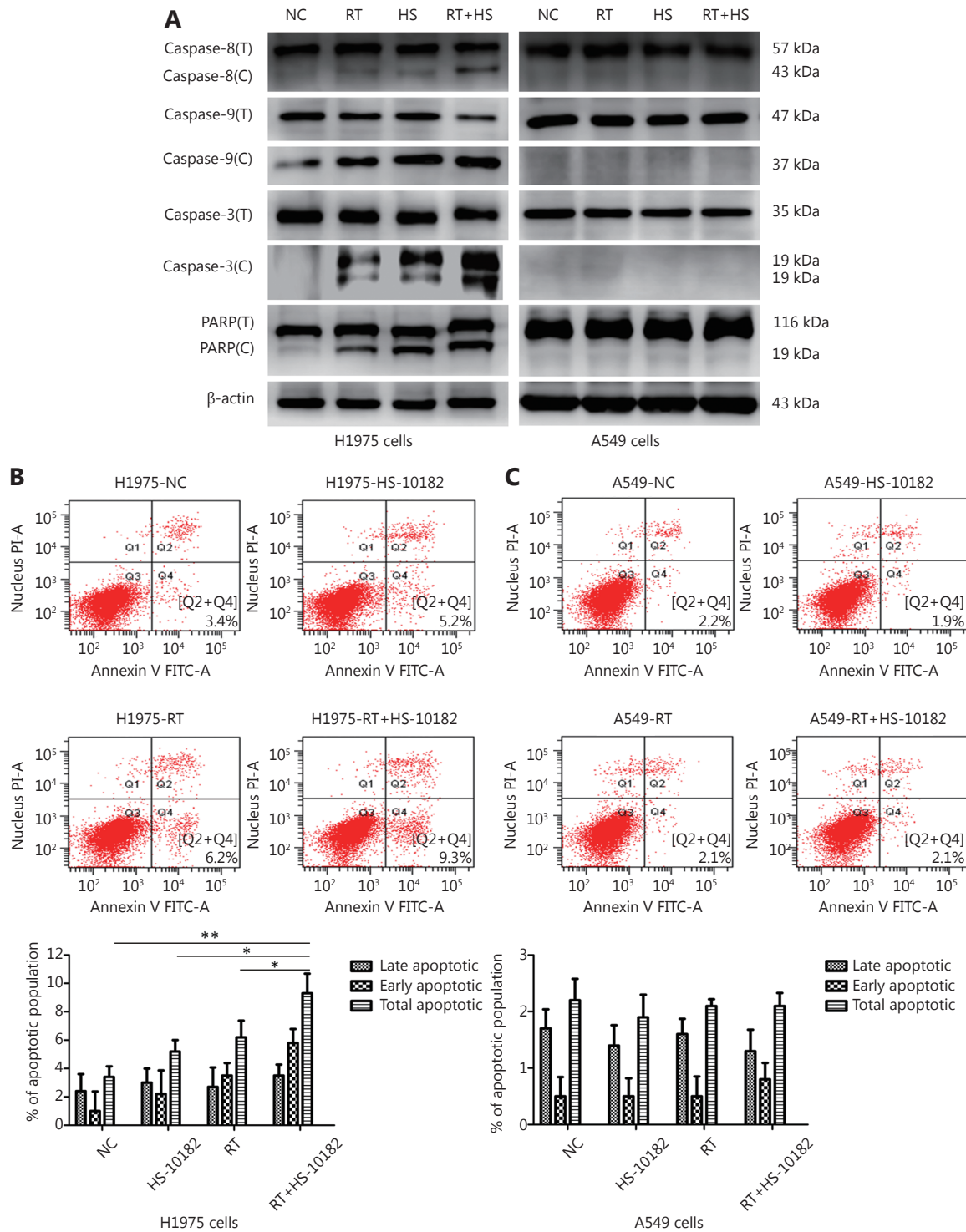


**Figure 3** HS-10182 enhances irradiation-induced apoptosis. (A) Lysates from H1975 and A549 cells treated with radiation (RT), HS-10182 (HS), or a combination of both (RT+HS) for 24 h were analyzed. Levels of cleaved caspase-8, caspase-9, caspase-3, and PARP were detected and compared with the total levels of each protein (labeled with C vs. T). Detection of  $\beta$ -actin was performed as a loading control. (B) Apoptosis was detected in the NC, RT, HS, and RT+HS samples of the H1975 and A549 cells via flow cytometry. (C) Quantification of the flow cytometry data according to apoptosis stage is shown with the error bars representing standard deviation values. \* $P < 0.05$ ; \*\* $P < 0.01$ , based on the Student's *t*-test.

8, caspase-9, caspase-3, and PARP increased following treatment with HS-10182 or radiation alone. An even greater increase was observed following exposure to both HS-10182 and radiation. In contrast, the levels of these proteins did not significantly change in the A549 cells. To further analyze which mechanism(s) are involved in this observed sensitization, the percentage of cells undergoing apoptosis following the various treatments was detected by flow cytometry (**Figure 3B** and **C**). A higher percentage of cells undergoing apoptosis was observed for the HS-10182 alone group as compared with the radiotherapy alone group. When HS-10182 and radiation were both applied, a significantly higher percentage of cells undergoing apoptosis was observed. In contrast, the percentage of cells undergoing apoptosis in the A549 cells did not significantly differ amongst the treatment groups. Thus, our results indicate that HS-10182 enhances irradiation-induced apoptosis in H1975 cells, but not in A549 cells.

### **HS-10182 enhances the extent of irradiation-induced DNA damage and delays DNA repair**

Several studies have reported that DNA damage repair mechanisms are downregulated when the sensitivity to radiation is enhanced<sup>11</sup>. A linear relationship between the number of  $\gamma$ -H2AX foci and DNA double-strand breaks (DSB) has also been observed<sup>12</sup>. For this study, IF was used to detect changes in  $\gamma$ -H2AX foci in both H1975 and A549 cells as a surrogate for monitoring DSB. Briefly, cells were exposed to 6 Gy of radiation and then subsequently stained with antibodies raised against  $\gamma$ -H2AX at various time points (e.g., 0, 1, 4, and 24 h after irradiation). The results are presented in **Figure 4** and they show that the number of  $\gamma$ -H2AX foci dramatically increased within 1 h of each cell line being exposed to 6 Gy of radiation, and then the numbers began to decrease. When the cells were treated with HS-10182 for 2 h before receiving 6 Gy radiation, a high number of  $\gamma$ -H2AX foci were observed in the H1975 cells 24 h after irradiation. However, in the A549 cells that underwent the same combination treatment, the number of  $\gamma$ -H2AX foci were reduced by 60% after 4 h, and at 24 h, the number of  $\gamma$ -H2AX foci suggested that DNA repair was nearly complete (**Figure 4C** and **D**). In addition, we validated the results of IF by Western blot experiments. The results show that the level of  $\gamma$ -H2AX dramatically increased within 1 h of each cell line being exposed to 6 Gy of radiation, a high level of  $\gamma$ -H2AX expression was observed in the H1975 cells 24 h after irradiation. However, in the A549 cells the level of  $\gamma$ -H2AX began to decrease 4 h after irradiation (**Figure 4E**). DNA-PKs

are key proteins in the nonhomologous end-joining (NHEJ) repair mechanism<sup>13</sup>. In the RT+HS group for the H1975 cells and A549 cells, the expression of the DNA-PKcs was detected and it was found to be significantly enhanced as compared to the RT group. Furthermore, the increased level of DNA-PKcs in the H1975 cells was more significant than that in the A549 cells. Based on these results, the combination treatment of HS-10182 and radiation appears to involve the NHEJ repair pathway. To gain further insight into the potential role of HS-10182 in irradiation-induced DNA damage, other DNA damage response proteins were examined. Specifically, Rad50 and Ku70 proteins were detected in Western blot. In the H1975 cells, expression of Rad50 was enhanced following RT, while a radiation-induced increase in its expression was not observed following treatment with HS-10182 and radiation. In contrast, the levels of Rad50 in A549 cells with no significant changes were observed in the different groups. When Ku70 levels were examined, no significant changes were observed in either the H1975 cells or the A549 cells after their treatments (**Figure 5A**). Additionally, we validated these results by IF. In the RT+HS group the expression of the DNA-PKcs was significantly enhanced as compared to the RT group in either the H1975 cells or the A549 cells. In the H1975 cells, the expression of Rad50 was enhanced following RT, but in the RT+HS group the expression of Rad50 was reduced as compared to the RT group. When the Rad50 level was examined in A549 cells, no significant changes were observed among different groups (**Figure 5B**). Taken together, these results suggest that HS-10182 can increase the extent of DNA damage and delay its repair following irradiation. Moreover, radiosensitization mediated by HS-10182 may involve a reduction in Rad50 expression.

### **Combination therapy with HS-10182 and radiation inhibits tumor growth**

A xenograft model was established to conduct *in vivo* studies regarding the effects of HS-10182 and radiation on tumor growth. Briefly, H1975 cells were injected into the right leg of female Nu/Nu mice (**Figure 6A**). After approximately six days, the average tumor volume reached 200 mm<sup>3</sup>. At this point, 24 mice were randomized into four groups to receive the following treatments: 1) no treatment [control group (NC)]; 2) HS-10182 (5 mg/kg per day for days 6–12); 3) RT (10 Gy over five fractions on days 8–12); and 4) RT (10 Gy over five fractions on days 8–12) + HS-10182 (5 mg/kg per day for days 6–12) (**Figure 6B**). For the radiation treatments, they were administered daily with a radiation dose of 2 Gy delivered to the right leg by a 6MV X-ray irradiator

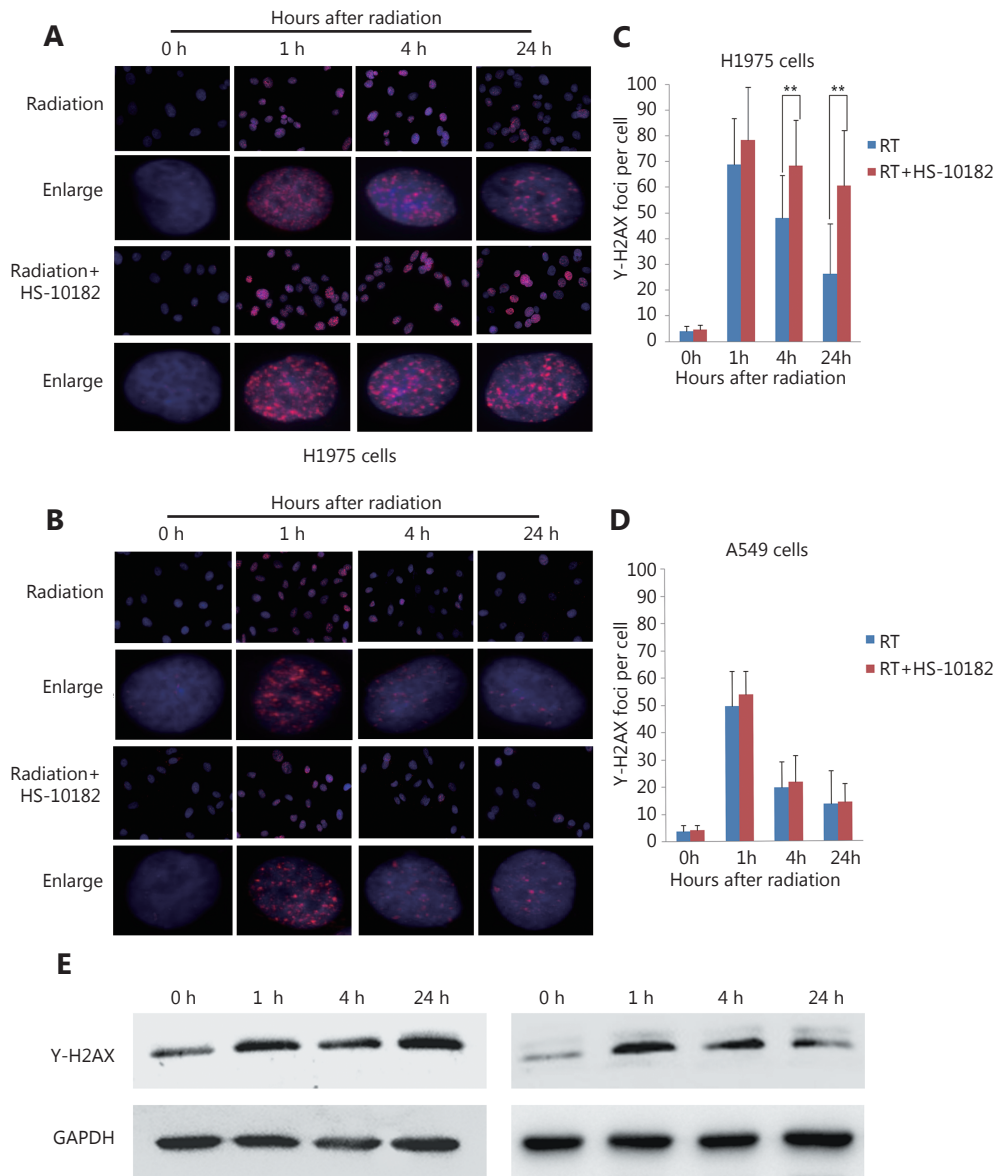


**Figure 4** HS-10182 enhances the extent of irradiation-induced DNA damage and delays DNA damage repair. (A, B) Immunofluorescence analyses were performed to examine changes in the formation of nuclear  $\gamma$ -H2AX foci in H1975 cells and A549 cells following treatment with radiation and radiation + HS-10182. Enlarged view shows the representative images of  $\gamma$ -H2AX foci in nuclei at 40 $\times$  magnification. The results are expressed as means  $\pm$  SD values in a minimum of 100 cells per treatment group. (C, D) Quantification of the average number of irradiation-induced  $\gamma$ -H2AX foci counted in H1975 cells and A549 cells. (E) Western blots were performed to examine changes in  $\gamma$ -H2AX foci in H1975 cells and A549 cells following treatment with radiation + HS-10182. Data represent the mean values from three independent experiments. \* $P < 0.05$ ; \*\* $P < 0.01$ , based on the Student's  $t$ -test.

(VARIAN 600CD) at a dose rate of 3 Gy/min. Treatment with HS-10182 enhanced the radiosensitivity of the H1975 xenografts, while the combination treatment of radiotherapy and HS-10182 significantly inhibited tumor growth as compared to HS-10182 or radiotherapy alone (Figure 6C and D).

### HS-10182 enhanced the radiosensitivity of the H1975 xenografts by increasing the degree of apoptosis and the extent of DNA damage

To further confirm the capacity of HS-10182 to enhance the radiosensitivity of the H1975 xenografts that were



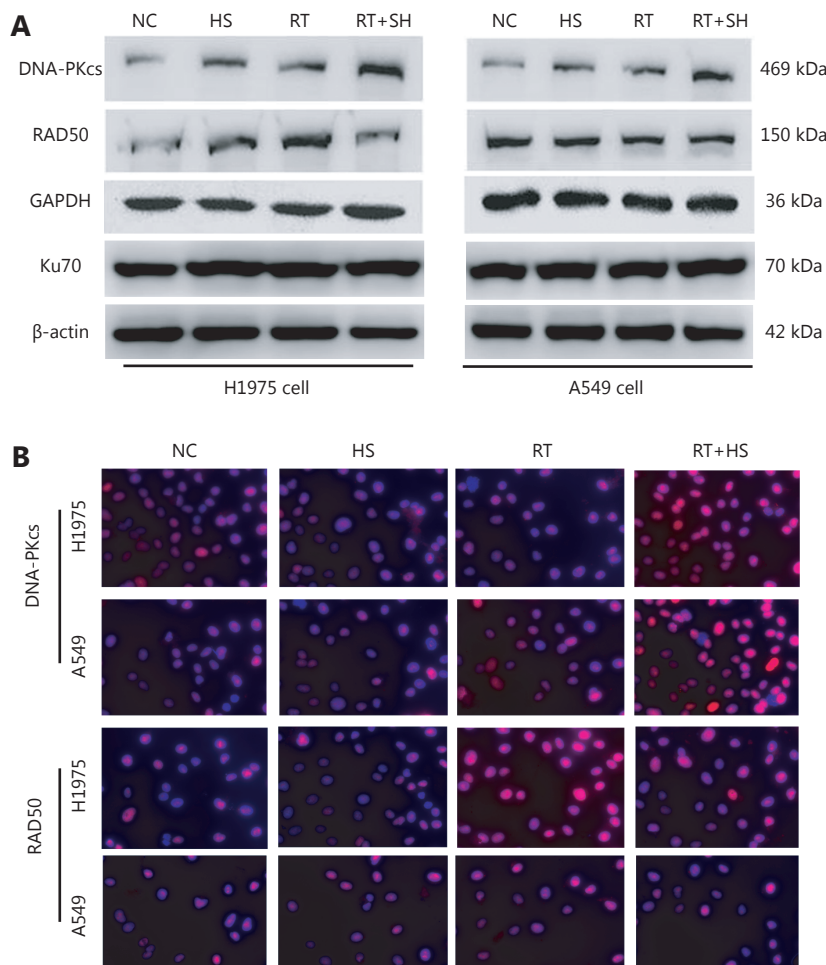


**Figure 5** Effect of HS-10182 on levels of DNA damage response proteins. (A) Total cell lysates were collected from H1975 and A549 cells that underwent treatment with HS-10182 (HS), radiation (RT), or a combination of both (RT+HS) for 24 h. Levels of DNA damage-related proteins were monitored (DNA-PKcs, Rad50, and Ku70 proteins). Detection of  $\beta$ -actin served as a loading control. (B) Immunofluorescence analyses were performed to examine changes of DNA-PKcs and Rad50 in H1975 cells and A549 cells following treatment with HS-10182, radiation, and radiation + HS-10182.

established, we assessed the levels of p-EGFR in the tumor tissues, as well as the proliferation marker, Ki-67, the apoptosis marker, cleaved caspase-3, and expression of the DNA damage markers, DNA-PKcs and Rad50. Levels of p-EGFR increased in the tissues that were analyzed from the RT group as compared with the tissues that were analyzed from the NC group, yet its levels were lower in the HS group as compared to the NC group. The levels of p-EGFR in the RT+HS group were also reduced as compared to the RT group. In contrast, the combination treatment led to a significant increase in the levels of cleaved caspase-3 and DNA-PKcs. Meanwhile, treatment with HS-10182 blocked an irradiation-induced increase in the expression of DNA-PKcs in the H1975 xenografts (**Figure 6E**).

## Discussion

For patients with NSCLC that has EGFR-activating mutations, treatment with an EGFR-TKI is a standard first-line therapy<sup>14</sup>. However, most patients who initially benefit from EGFR-targeted therapies eventually develop resistance<sup>15</sup>. Moreover, approximately 60% of these patients' mechanism of resistance involves the EGFR T790M mutation<sup>16</sup>. As chemotherapy has no effect on patients with EGFR-mutant lung cancers with acquired resistance to TKIs<sup>17</sup>, approximately 50% of cancer patients will receive radiotherapy during their treatment course. Despite radical radiotherapy, however, 20%–44% of patients will develop loco-regional progression after two years<sup>18</sup>. Therefore, an

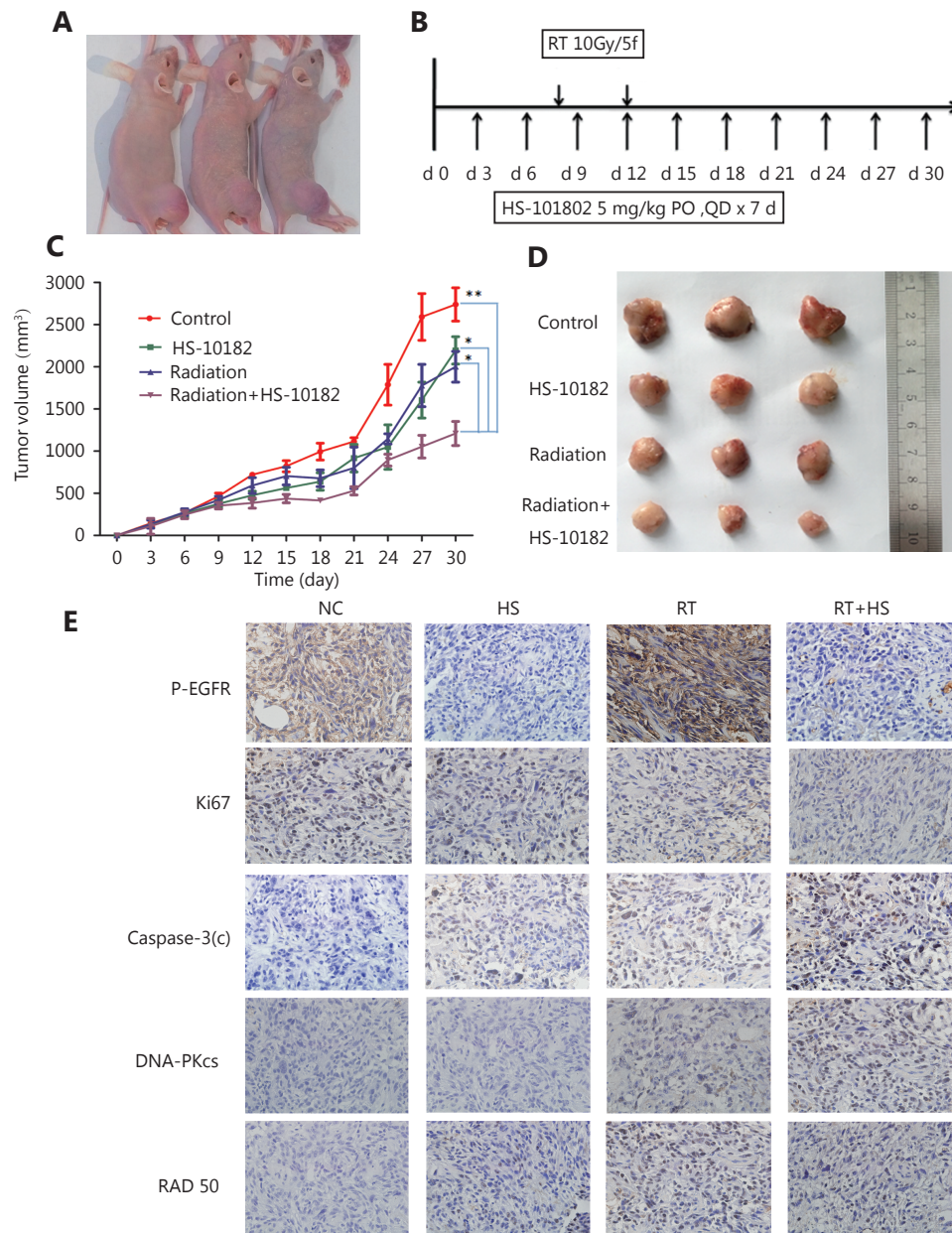


**Figure 6** Effect of HS-10182 *in vivo*. (A) Xenograft models were established following the injection of cells into the right leg of Nu/Nu mice. (B) Timeline of the treatment schedule. (C) Tumor growth was measured three times a week for each treatment group. The growth curves represent the average tumor volume values for six mice in each group. Error bars represent the standard deviation values. \* $P < 0.05$ ; \*\* $P < 0.01$ , based on the Student's *t*-test. (D) Images of representative tumors resected from mice in the four treatment groups. (E) After 14 days of treatment with HS-10182 (HS), radiation (RT), or a combination of both (RT+HS), xenograft tumor tissues were collected from the four treatment groups and subjected to immunostaining assays to detect changes in levels of p-EGFR, Ki67, cleaved caspase-3, DNA-PKcs, and Rad50 (IHC staining, 400  $\times$ ).

ability to increase the sensitivity of tumors to radiotherapy and increase tumor control is greatly needed.

A number of studies have reported that radiation activates EGFR signaling, and this leads to radioresistance that is

mediated via induced cell proliferation and enhanced DNA repair<sup>19</sup>. In preclinical studies, EGFR-TKIs have enhanced the radiation response at the cellular level by affecting cell cycle arrest, the induction of apoptosis, the acceleration of cellular

repopulation, and DNA damage repair<sup>20</sup>. In clinical studies, radiation combined with EGFR-TKIs have inhibited tumor proliferation, increased apoptosis, prolonged G2/M arrest, and significantly enhanced DNA injury in colorectal cancers<sup>21</sup>. In particular, gefitinib has exhibited a radiosensitizing effect on cell lines and has been investigated in combination with RT for unresectable stage III NSCLC<sup>19</sup>. In the present study, the effects of HS-10182 on the radiosensitivity of NSCLC cells were investigated.

Caspase-8 functions in a mitochondria-dependent manner via caspase-9 to initiate apoptosis<sup>22</sup>. Thus, activation of caspase-9 can represent an indirect marker of apoptosome formation. Activated caspase-9 also activates the downstream executioner protein, caspase-3<sup>10</sup>, which plays a critical role during apoptosis<sup>23</sup>. Activated caspase-3 induces the cleavage and activation of PARP proteins, which is another useful marker of apoptosis<sup>24</sup>. In the present study, levels of cleaved caspase-8, caspase-9, caspase-3, and PARP were higher following the combination treatment of HS-10182 and radiation in H1975 cells. However, the levels of these four proteins remained essentially unchanged in the A549 cells. When apoptosis was detected in the different treatment groups by flow cytometry, the same results were obtained. Therefore, the combination of HS-10182 treatment and radiation appears to enhance apoptosis in NSCLC cells that carry a T790M mutation in EGFR, while this combined treatment did not enhance apoptosis in NSCLC cells expressing wild-type EGFR.

DNA is directly susceptible to radiation and DNA DSBs that occur because of this radiation are among the most dangerous lesions. DNA-PKcs is a member of the phosphatidylinositol-3 kinase (PI3K)-related protein kinase family and it has a critical role in the NHEJ pathway of DSB repair<sup>25</sup>. The greater the number of DNA DSBs that are present in a genome the greater the number of DNA-PKcs proteins that are required to repair them. In the present study, the levels of DNA-PKcs were enhanced after the combination treatment in both the H1975 cells and the A549 cells, with the level of DNA-PKcs being higher in the H1975 cells. Taken together, these results indicate the potential of HS-10182 to enhance the degree of irradiation-induced DNA damage.

In previous studies,  $\gamma$ -H2AX has been related to DNA-dependent processes such as repair, replication, recombination, and transcription<sup>26</sup>. Thus, the number of  $\gamma$ -H2AX foci is considered a marker of DSBs, with each DSB potentially yielding one focus. Therefore,  $\gamma$ -H2AX foci have been used to monitor DSBs<sup>27</sup>. In a clinical study, a  $\gamma$ -H2AX assay exhibited potential as a screening tool for evaluating the

radiosensitivity of individual breast cancer patients<sup>28</sup>. In the present study, the H1975 cells that were treated with HS-10182 had a greater number of  $\gamma$ -H2AX foci, and this number was maintained for up to 24 h after irradiation. These data further validate the capacity of HS-10182 to enhance radiosensitivity by inducing DNA damage and causing a delay in its repair.

Rad50 is a member of the structural maintenance of chromosomes (SMC) family of proteins and is essential for cell growth and viability<sup>29</sup>. In particular, it has been demonstrated that Rad50 is involved in: chromosome organization, protection of chromosomes ends, and maintenance of genomic integrity<sup>30</sup>. Rad50 forms a complex with Meiotic recombination 11 (MRE11) and Nijmegen Breakage Syndrome 1 (NBS1) referred to as the MRE11-RAD50-NBS1 (MRN) complex and acts in the initial stages of DSB repair. Rad50 is also one of the first proteins to detect the DNA ends that are created at DSBs, while the MRN complex affects homologous recombination repair (HRR) and NHEJ pathways<sup>31</sup>. After the combination treatment in the present study, expression of Rad50 was reduced in the H1975 cells, indicating that HS-10182 may affect chromosome stability and further influence cell growth and viability. It is generally assumed that chromosomal abnormalities inhibit the activity of cancer cells by interrupting their growth. It is also possible that HS-10182 suppressed an increase in Rad50 expression in response to irradiation, thereby compromising the activity of the HRR and NHEJ repair pathways and increasing radiosensitivity.

When HS-10182 was applied to a xenograft model of H1975 cells, the combination treatment resulted in a significant inhibition of tumor growth as compared with the administration of HS-10182 or radiation alone. Moreover, in the immunohistochemical assays with these tumor tissues that were performed following the treatment, the data regarding proliferation, apoptosis, and DNA damage markers were in agreement with the data obtained *in vitro*.

To our knowledge, we have demonstrated in the present study for the first time that HS-10182 can significantly enhance the radiosensitivity of NSCLCs that carry an EGFR T790M mutation. A possible mechanism involves the ability of HS-10182 to enhance irradiation-induced apoptosis, to increase irradiation-induced DNA damage, and to delay DNA damage repair. Consequently, HS-10182 may also affect chromosome stability. Additional research is needed to confirm the present findings and to further investigate chromosome stability. However, the present findings suggest that radiotherapy combined with HS-10182 represents a novel treatment for lung cancer cells which have acquired an

EGFR T790M mutation and the translation of this approach to increase radiosensitivity in the clinical setting may hold great promise.

## Acknowledgments

This work was supported by the National Natural Science Foundation of China (Grant No. 81372518) and the Tianjin Key Problem Tackling Project for Cancer Therapy (Grant No. 12ZCDZSY15900).

## References

- Singh D, Attri BK, Gill RK, Bariwal J. Review on EGFR inhibitors: critical updates. *Mini Rev Med Chem*. 2016; 16: 1134-66.
- Eke I, Schneider L, Forster C, Zips D, Kunz-Schughart LA, Cordes N. EGFR/JIP-4/JNK2 signaling attenuates cetuximab-mediated radiosensitization of squamous cell carcinoma cells. *Cancer Res*. 2013; 73: 297-306.
- Yarden Y, Sliwkowski MX. Untangling the ErbB signalling network. *Nat Rev Mol Cell Biol*. 2001; 2: 127-37.
- Kasten-Pisula U, Saker J, Eicheler W, Krause M, Yaromina A, Meyer-Staeckling S, et al. Cellular and tumor radiosensitivity is correlated to epidermal growth factor receptor protein expression level in tumors without *EGFR* amplification. *Int J Radiat Oncol Biol Phys*. 2011; 80: 1181-8.
- Siegel R, Ma JM, Zou ZH, Jemal A. Cancer statistics, 2014. *CA Cancer J Clin*. 2014; 64: 9-29.
- Tyldesley S, Boyd C, Schulze K, Walker H, Mackillop WJ. Estimating the need for radiotherapy for lung cancer: an evidence-based, epidemiologic approach. *Int J Radiat Oncol Biol Phys*. 2001; 49: 973-85.
- Zhou L, He JZ, Xiong WJ, Liu YM, Xiang J, Yu Q, et al. Impact of whole brain radiation therapy on CSF penetration ability of Icotinib in *EGFR*-mutated non-small cell lung cancer patients with brain metastases: results of phase I dose-escalation study. *Lung Cancer*. 2016; 96: 93-100.
- Kriegs M, Gurtner K, Can Y, Brammer I, Rieckmann T, Oertel R, et al. Radiosensitization of NSCLC cells by EGFR inhibition is the result of an enhanced p53-dependent G1 arrest. *Radiother Oncol*. 2015; 115: 120-7.
- Xu P, Zhang WB, Cai XH, Qiu PY, Hao MH, Lu DD. Activating AKT to inhibit JNK by troxerutin antagonizes radiation-induced PTEN activation. *Eur J Pharmacol*. 2016; 795: 66-74.
- Mondal A, Bennett LL. Resveratrol enhances the efficacy of sorafenib mediated apoptosis in human breast cancer MCF7 cells through ROS, cell cycle inhibition, caspase 3 and PARP cleavage. *Biomed Pharmacother*. 2016; 84: 1906-14.
- Zhang D, Wang HB, Sun ME, Yang J, Zhang W, Han SX, et al. Speckle-type POZ protein, SPOP, is involved in the DNA damage response. *Carcinogenesis*. 2014; 35: 1691-7.
- Leatherbarrow EL, Harper JV, Cucinotta FA, O'Neill P. Induction and quantification of  $\gamma$ -H2AX foci following low and high LET-irradiation. *Int J Radiat Biol*. 2006; 82: 111-8.
- Sun XN, Yang CY, Liu H, Wang Q, Wu SX, Li X, et al. Identification and characterization of a small inhibitory peptide that can target DNA-PKcs autophosphorylation and increase tumor radiosensitivity. *Int J Radiat Oncol Biol Phys*. 2012; 84: 1212-9.
- Hoshi H, Hiyama G, Ishikawa K, Inageda K, Fujimoto J, Wakamatsu A, et al. Construction of a novel cell-based assay for the evaluation of anti-EGFR drug efficacy against EGFR mutation. *Oncol Rep*. 2017; 37: 66-76.
- Yu HA, Arcila ME, Rekhtman N, Sima CS, Zakowski MF, Pao W, et al. Analysis of tumor specimens at the time of acquired resistance to EGFR-TKI therapy in 155 patients with *EGFR*-mutant lung cancers. *Clin Cancer Res*. 2013; 19: 2240-7.
- Chong CR, Jänne PA. The quest to overcome resistance to EGFR-targeted therapies in cancer. *Nat Med*. 2013; 19: 1389-400.
- Johnson ML, Riely GJ, Rizvi NA, Azzoli CG, Kris MG, Sima CS, et al. Phase II trial of dasatinib for patients with acquired resistance to treatment with the epidermal growth factor receptor tyrosine kinase inhibitors erlotinib or gefitinib. *J Thorac Oncol*. 2011; 6: 1128-31.
- Vansteenkiste J, De Ruyscher D, Eberhardt WE, Lim E, Senan S, Felip E, et al. Early and locally advanced non-small-cell lung cancer (NSCLC): ESMO Clinical Practice Guidelines for diagnosis, treatment and follow-up. *Ann Oncol*. 2013; 24(Suppl 6): vi89-98.
- Provencio M, Sánchez A, Garrido P, Valcárcel F. New molecular targeted therapies integrated with radiation therapy in lung cancer. *Clin Lung Cancer*. 2010; 11: 91-7.
- Chinnaiyan P, Huang S, Vallabhaneni G, Armstrong E, Varambally S, Tomlins SA, et al. Mechanisms of enhanced radiation response following epidermal growth factor receptor signaling inhibition by erlotinib (Tarceva). *Cancer Res*. 2005; 65: 3328-35.
- Ma H, Bi JP, Liu T, Ke Y, Zhang S, Zhang T. Icotinib hydrochloride enhances the effect of radiotherapy by affecting DNA repair in colorectal cancer cells. *Oncol Rep*. 2015; 33: 1161-70.
- Wu YQ, Zhao D, Zhuang JB, Zhang FQ, Xu C. Caspase-8 and Caspase-9 functioned differently at different stages of the cyclic stretch-induced apoptosis in human periodontal ligament cells. *PLoS One*. 2016; 11: e0168268
- Srivastava SK, Bhardwaj A, Arora S, Tyagi N, Singh S, Andrews J, et al. MicroRNA-345 induces apoptosis in pancreatic cancer cells through potentiation of caspase-dependent and-independent pathways. *Br J Cancer*. 2015; 113: 660-8.
- Xu P, Cai XH, Zhang WB, Li YN, Qiu PY, Lu DD, et al. Flavonoids of *Rosa roxburghii* Tratt exhibit radioprotection and anti-apoptosis properties via the Bcl-2(Ca<sup>2+</sup>)/Caspase-3/PARP-1 pathway. *Apoptosis*. 2016; 21: 1125-43.
- Yu L, Shang ZF, Hsu FM, Zhang Z, Tumati V, Lin YF, et al. NSCLC cells demonstrate differential mode of cell death in response to the combined treatment of radiation and a DNA-PKcs inhibitor. *Oncotarget*. 2015; 6: 3848-60.

26. Singh I, Ozturk N, Cordero J, Mehta A, Hasan D, Cosentino C, et al. High mobility group protein-mediated transcription requires DNA damage marker  $\gamma$ -H2AX. *Cell Res.* 2015; 25: 837-50.
27. Johansson P, Fasth A, Ek T, Hammarsten O. Validation of a flow cytometry-based detection of  $\gamma$ -H2AX, to measure DNA damage for clinical applications. *Cytometry Part B Clin Cytom.* 2017; 92: 534-40.
28. Djuzenova CS, Elsner I, Katzer A, Worschech E, Distel LV, Flentje M, et al. Radiosensitivity in breast cancer assessed by the histone  $\gamma$ -H2AX and 53BP1 foci. *Radiat Oncol.* 2013; 8: 98
29. Kinoshita E, van der Linden E, Sanchez H, Wyman C. RAD50, an SMC family member with multiple roles in DNA break repair: how does ATP affect function? *Chromosome Res.* 2009; 17: 277-88.
30. Laffitte MCN, Leprohon P, Hainse M, Légaré D, Masson JY, Ouellette M. Chromosomal translocations in the parasite leishmania by a MRE11/RAD50-independent microhomology-mediated end joining mechanism. *PLoS Genet.* 2016; 12: e1006117
31. Hohl M, Kwon Y, Galván SM, Xue XY, Tous C, Aguilera A, et al. The Rad50 coiled-coil domain is indispensable for Mre11 complex functions. *Nat Struct Mol Biol.* 2011; 18: 1124-31.

**Cite this article as:** Chen Y, Wang Y, Zhao L, Wang P, Sun J, Bao R, et al. EGFR tyrosine kinase inhibitor HS-10182 increases radiation sensitivity in non-small cell lung cancers with EGFR T790M mutation. *Cancer Biol Med.* 2018; 15: 39-51. doi: 10.20892/j.issn.2095-3941.2017.0118